RESEARCH NOTE

A NUMERICAL STUDY OF SINGLE-PHASE FORCED CONVECTIVE HEAT TRANSFER WITH FLOW FRICTION IN MICROCHANNELS

P. Mohajeri Khameneh*

Department of Mechanical Engineering, Bandar Lengeh Branch, Islamic Azad University, Bandar Lengeh, Iran
pedram.mohajeri@gmail.com

I. Mirzaie, N. Pourmahmoud, S. Majidyfar

Department of Mechanical Engineering, Faculty of Engineering, Urmia University, Urmia, Iran
enpim@yahoo.com, n.pormahmoud@urmia.ac.ir, samad_majidyfar@yahoo.com

S.H. Azizi, M.R. Andalibi

Department of Mechanical Engineering, Bandar Lengeh Branch, Islamic Azad University, Bandar Lengeh, Iran
s.hossein.azizi@gmail.com, andalibi.mr@hotmail.com

*Corresponding Author

(Received: January 01, 2011 – Accepted in Revised Form: December 15, 2011)

doi: *10.5829/idosi.ije.2012.25.01a.08*

Abstract Three-dimensional simulations of the single-phase laminar flow and forced convective heat transfer of water in microchannels with small rectangular sections having specific hydraulic diameters and distinct geometric configurations were investigated numerically. The numerical results indicated that the laminar heat transfer was to be dependent upon the aspect ratio and the ratio of the hydraulic diameter to the center to center distance of the microchannels. The geometries and operating conditions of that indicated microchannel were created using a finite volume-based computational fluid dynamics technique. The aim of this paper is to obtain computational Nusselt number in laminar flow using Fluent CFD Solver and to validate it with available experimental studies. Acquired numerical results have an admissible compatibility with available experimental studies. In addition, conceivable temperature profiles and pressure drops have been obtained at each Z-location in this model. Then, pressure drop values in the present model were explored for each Reynolds number. Finally, the effects of geometric parameters on the average Nusselt number in the laminar flow were illustrated numerically.

Keywords Heat transfer; Pressure drop; Laminar flow; CFD; Nusselt number.

چکیده شبیه سازی‌های سه بعدی انتقال حرارت جابه جایی اجباری در رژیم جریان آرام برای سیال آب تک فازی در میکروکانال‌هایی با مقاطع مستطیلی کوچک و قطر هیدرولیکی مشخص و آرایش هندسی متفاوت، به صورت عددی مورد بررسی قرار گرفته است. نتایج عددی نشان دهنده‌ی این است که انتقال حرارت در رژیم جریان آرام به نسبت "طول به عرض" و نسبت "قطر هیدرولیکی به فاصله‌ی مرکز تا مرکز دریچه‌ی میکروکانال‌ها" وابسته است. هندسه و شرایط عملکردی میکروکانال مذکور توسط نرم افزار تحلیل سیالاتی فلوئنت مورد بررسی واقع شده است. در مقاله حاضر، عدد نوسلت محاسباتی در جریان آرام توسط روش‌های عددی محاسبه و نتایج عددی برای صحه‌گذاری با نتایج تجربی مقایسه شده است و این‌گونه نتیجه شد که نتایج عددی و تجربی همخوانی و سازگاری قابل قبولی با یکدیگر دارند. سپس در هر یک از موقعیت‌های عمق کانال (Z) برای هر یک از شبیه‌سازی‌های انجام شده، پروفیل‌های دمایی و افت فشارها ترسیم شده است. نهایتاً، اثر پارامترهای هندسی روی عدد نوسلت میانگین گیری شده در رژیم جریان آرام به صورت عددی مورد بررسی قرار گرفته است.

1. INTRODUCTION

Microchannel structures are utilized widely for more than 20 years in miscellaneous industries. These systems are used by manufacturers who wanted efficient heat exchange in a compact design. Today, the advantages of microchannel systems are beginning to challenge traditional coil technology in different manufactures. As an example, The air conditioning industry faces a continuous challenge to provide higher efficiency levels and greater equipment reliability. This challenge is even more difficult to meet when the aim is simultaneously to maintain equipment size and reduce potential cost influence. Previous engineering solutions designed to compensate these requirements have typically included such changes as improving individual components or increasing the overall heat transfer surface area to increase thermal efficiency. However, each of these improvements tends to increase equipment size, cost, or both. An optional solution for air conditioning applications is microchannel heat exchanger technology. This heat exchanger technology has been widely used in the automotive industry for many years, with considerable success [1].

The importance of convective heat transfer in microchannel structures has increased dramatically because of practical applications involving the thermal control of electronic devices. In the earliest investigation of microscale flow and heat transfer, Tuckermann and Pease [2] studied the fluid flow and heat transfer characteristics in microchannels, and demonstrated that electronic chips could be effectively cooled by means of the forced convective flow of water through microchannels fabricated either directly in the silicon wafer or in the circuit board on which the chips were mounted. Since this initial study other investigations have supported the earliest findings and have served to illustrate the unusually high levels of heat removal that can be accomplished using microchannel structures [3].

Shortly after the initial work of Tuckermann et al. [2, 3], Wu and Little [4, 5] measured the flow friction and heat transfer characteristics of gases flowing through microchannels and observed that the convective heat transfer characteristics departed from the typical experimental results for conventionally sized channels. Other investigations by Choi et al. [6], Weisberg et al. [7] and Bowers and Mudawar [8] all provided additional information and considerable evidence that the behavior of fluid flow and heat transfer in microchannels or microtubes is substantially different from that which typically occurs in larger channels or tubes. In an attempt to clarify some of the questions surrounding this issue, Peng and Wang [9] and Peng et al. [10] investigated microchannel structures. In these investigations the heat transfer and flow mode conversions for single phase forced convection in microchannels were studied. Peng and Peterson [11] analyzed experimentally the effects of thermofluid and the geometric variables on the heat transfer using methanol flowing through microchannel structures. Peng et al. [12, 13] measured both the flow friction and the heat transfer for single phase convection in an array of parallel microchannels.

A numerical study about three-dimensional fluid flow and heat transfer in a rectangular microchannel heat sink was analyzed numerically using water as the cooling fluid by Qu and Mudawar. One of their major goal was to present a detailed description of the local and average heat transfer characteristics, i.e. temperature, heat flux, and Nusselt number in microchannel heat sinks. From their investigation it was found that the highest temperature is encountered at the heated base surface of the heat sink immediately above the channel outlet and also it was stated that the heat flux and Nusselt number have much higher values near the channel inlet and vary around the channel periphery, approaching zero in the corners [14].

Therefore, a comprehensive review was presented on the investigations of the forced single-phase convective heat transfer in non-circular microchannels by Peng et al. [15]. In their literature the observations and results available in the open literature are inspected and compared for better understanding of the physical nature of the heat transfer performance. From their investigations it is concluded that appropriate data reduction and the correlating parameters will be the basis of comparability and evaluation for comprehensive investigations.

Consequently, the heat transfer characteristics of single-phase forced convection of R134a through single circular micro-channels with 1.7, 1.2, and 0.8 mm as inner diameters were investigated

experimentally by Owhaib and Palm [16]. The results were compared both to correlations for the heat transfer in macroscale channels and to correlations suggested for microscale geometries. The results show good agreement between the classical correlations and the experimentally measured data in the turbulent region. In the laminar regime, the heat transfer coefficients were almost identical for all three diameters.

Lately, a heat transfer analysis and comparison between conventional size formulations and microchannel size investigations were conducted by Mokrani et al. [17]. The main conclusion of this study is that the conventional size correlations are feasible to the microchannels with heights in a range of 50 to 500 microns. In addition, it was shown that the transition from laminar to turbulent regime is occurred in those two indicated structuresin a similar manner.

The present work was taken on to compare computational Nusselt number with available experimental results. After that, the effects of pressure drop along the microchannels on average Nusselt number was explored at each simulation. Finally, the influence of the geometric parameters on the average Nusselt number was investigated numerically.

2. NUMERICAL ANALYSIS

2.1. Description Of The Model In this paper, the fluid flow and heat transfer in a three-dimensional symmetric microchannel is simulated numerically. in order to validate this numerical study a reliable experimental study is necessitated. With utilizing of this experimental study, the suitability of these numerical simulations in investigation of thermal efficiency in laminar region will be authenticated. Hence, Peng and Peterson's experimental correlation [18], equation 1, was utilized in order to confirmed this numerical simulation.

$$Nu = 0.1165(\frac{D_h}{W_c})^{0.81}(\frac{H}{W})^{-0.79} Re_{D_h}{}^{0.62} Pr_f{}^{1/3} \quad (1)$$

Twelve different plates from the standpoint of geometric characteristics were utilized in Peng and Peterson's experimental investigation [18]. The hydraulic diameter of these plates are varied between 0.15 to 0.343 mm. In all these experiments single phased water was used as an operating fluid. In Figure 1, which it is exhibited in Peng and Peterson's article [18], calculated experimental Nusselt numbers including traced form of equation 1 are demostrated.

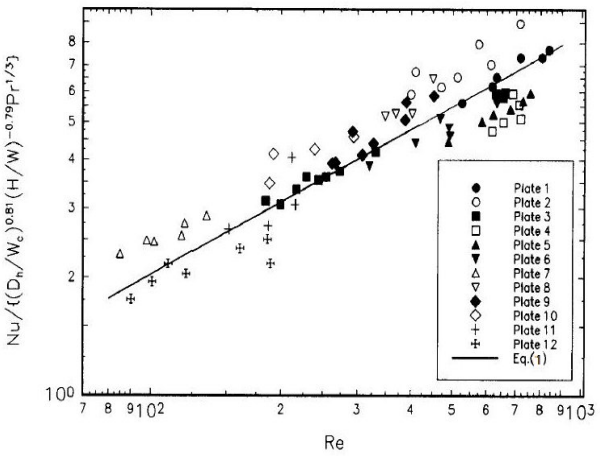

Figure 1. Peng and Peterson's Experimental Results of laminar heat transfer

As it can be seen in Figure 1, at the range of Reynolds number between 200 to 300, "Plate 3" has the most congruency with equation 1, which it is shown with a drawn line. Therefore, in order to validate coming numerical simulations, plate 3's geometry and operational characteristics will be exerted in the present range of Reynolds number. In this paper five simulations in the range of 200 to 300 Reynolds number are simulated and then the precision of obtained numerical results will be approved with Peng and Peterson's experimental results [18].

2.2 Assumptions Of Physical Model An isometric schematic and cross-section of the microchannel structure used in this investigation are shown in Figures 2, 3. During design process of this numerical model and by using symmetry conditions in some distinct faces, the calculative capability will be increased dramatically. Meanwhile, geometry parameters of this model are presented in Table 1. This microchannel plate dimensions are declared with microchannel width (W), microchannel height (H), center to center distance of microchannels (W_c), overall width (W_t) and overall length (L).

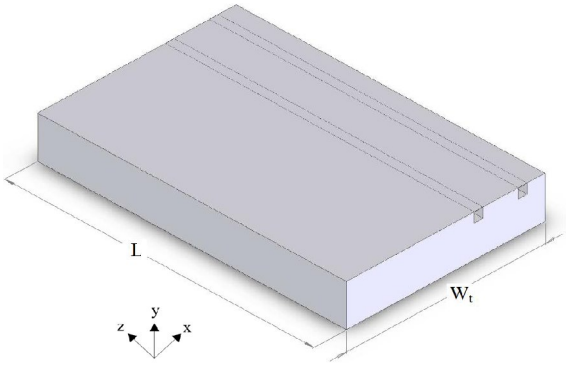

Figure 2. Isometric schematic of microchannel structure and the coordinate system

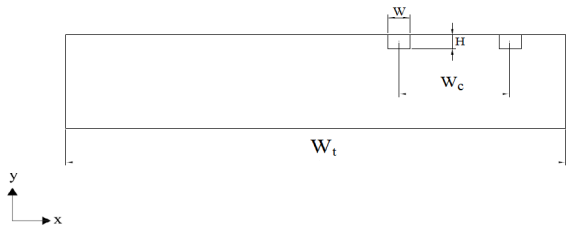

Figure 3. Cross-section of microchannel structure

TABLE 1. Geometric parameters for microchannel

Parameter	Length (mm)
W	0.4
H	0.3
W_c	2
W_t	18
L	45

During the meshing procedure of this existing model and in order to increase the calculative capability, compact grids are applied in channel volume and on the other hand harsh grids are exerted in all remainder parts of this model. Figure 4 clarify the sectional geometry and meshing grids of this numerical model clearly.

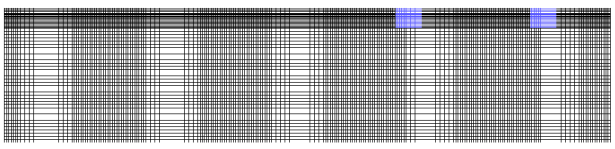

Figure 4. Sectional geometry and grid generated of plate3

Moreover, in order to gain confidence that all these numerical results aren't affiliated to different grid dimensions after exertion of meshing process, a grid independence examination is performed in this three dimensional model. In this study, based on number of grids which are available during the meshing procedure, three kind of grid qualities (rough, mediocre and harsh) were generated. After comparing iteration results and convergance speed, between these three kind of grids "mediocre meshing" is selected as a base model in order to continue further investigations and iterations in this numerical simulation.

The simulations were conducted according to the following assumptions:

1. In order to describe fluid flow and heat transfer in this physical model, three dimensional Navier-Stokes and energy equations were utilized.
2. The process is steady and the fluid is incompressible.
3. The flow is laminar.
4. The body forces are neglected.
5. The side walls and the top wall of the microchannel structure are adiabatic.
6. Radiation heat transfer and natural convective heat transfer are neglected.

2.3 Governing Equations And Boundary Conditions According to the above assumptions, the Navier-Stokes and energy equations are utilized to describe the fluid flow and heat transfer in the whole region including fluid and solid. The governing equations are:

Continuity:

$$\nabla.(\rho_f \vec{V}) = 0 \quad (2)$$

Momentum:

$$\nabla.(\rho_f \vec{V}\vec{V}) = -\nabla P + \nabla.(\mu_f \nabla \vec{V}) \quad (3)$$

Energy:

$$\nabla.(\vec{V}(\rho_f c_{p,f} T)) = \nabla.(k_f \nabla T) \quad (4)$$

where k_f , $\mu_f, \rho_f, c_{p,f}$ represent the thermal conductivity of water, molecular viscosity, density and specific heat at constant pressure of water flow, respectively.

In Fluent CFD Solver for this existing model,

"Mass flow inlet" and "Pressure outlet" are utilized as inlet and outlet boundary conditions, respectively. Meanwhile, in order to complete simulation of this model, "Symmetry" option is exerted for pre-defined sectional walls. Finally, after allocating all the "boundary conditions" and "Continuum types" in Fluent CFD Solver, this existing model is ready for numerical simulation procedure and iteration process.

2.4 Numerical Method In this numerical simulation procedure, five different simulations at the range of Reynolds number between 200 to 300 are investigated. At first, in order to determining the water mass flow rate ($\dot{m}$), equation (5) is exerted.

$$\dot{m} = \frac{ReA_{port}\mu}{D_h} \tag{5}$$

In order to locate D_h in equation 5, the value of hydraulic diameter is calculated with using of equation 6, as follows:

$$D_h = \frac{4(cross-section-area)}{Wetted-perimeter} = \frac{2W.H}{W+H} \tag{6}$$

The Darcy–Weisbach formulation, Equation 7, which it is presented in "Introduction to Heat Transfer" [19], will be utilized to determine pressure drop in laminar region of fluid flow. By placing Darcy friction factor *(f)* in equation (7), pressure outlets are calculated for each simulation.

$$\Delta p = f.\frac{L}{D_h}.\frac{\rho V^2}{2} \tag{7}$$

Above procedure for calculating pressure drops present admissible results. In Table 2, boundary conditions for each simulations are presented.

TABLE 2. Boundary conditions for each simulations

Simulation	Re_{Dh}	$\dot{m}$	P_{gauge}Pa
1	200	6.07E-05	7534.86
2	225	7.53E-05	8238.39
3	250	8.66E-05	9524.11
4	275	9.37E-05	10235.53
5	300	1.79E-04	10465.07

In Peng and Peterson's experimental study [18], their experimental model is heated with an electric heater which it has a low voltage *(V)* and high electric current *(I)*. This existing model has an uniform cross section and so, uniform heat flux is supposed during these simulations. In order to calculate the value of heat flux, the following correlation, equation 8, will be applied.

$$q'' = \frac{Q}{A_{plate}} \tag{8}$$

Meanwhile, in order to calculate total heat input *(Q)* and the area of the plate *(A_{plate})*, these following equations, equations 9 , 10, will be exerted as follows:

$$Q = I \times V \tag{9}$$

$$A_{plate} = W_t \times L \tag{10}$$

In Peng and Peterson's experimental study [18], values for electric current and voltage are presented as, *I=60A* and *V=0.20V*. By using equations 8, 9, 10, the value for the uniform heat flux which is exerted to the lower surface of this existing model will be calculated as, $q''=14814.81 \frac{W}{m^2}$.

After applying all the boundary conditions to this existing model, numerical simulations and iteration procedures will be performed. In Fluent CFD Solver, 10^{-3} residual convergence for continuity and momentum equations and 10^{-6} residual convergence for energy equation were contemplated. In the following sections, obtained numerical results will be compared with this available experimental study [18] and finally all the conclusions will be presented in detail.

3. RESULTS AND DISCUSSION

3.1. Model Validation The major goal in this section is to evaluate average Nusselt number in Fluent CFD Solver. Then, an exact comparison between obtained numerical results and Peng et al.'s experimental study [18] will be performed. One of the most important aims in this simulation is to calculate wall and fluid temperature at each Z-location in the depth of this model. In this three dimensional numerical simulation with utilizing "X-Y plot" option in Fluent CFD Solver, the trend of variations for wall and fluid temperature are calculated. Finally, after averaging the results in

Microsoft Excel at each Z location, temperature profiles for wall and water fluid are acquired. Wall and water fluid temperatures at each Z- locations are shown in Figure 5.

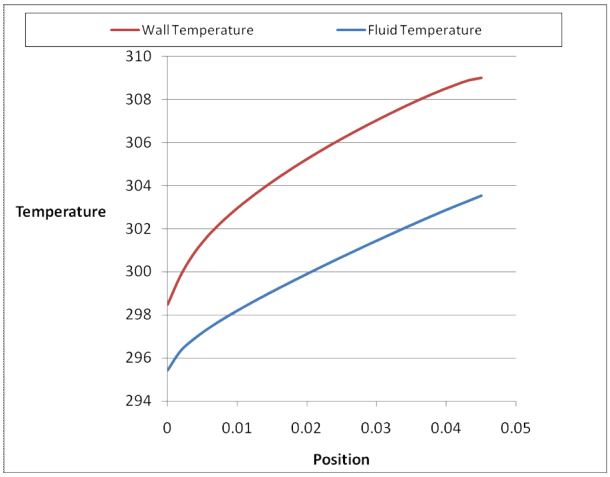

Figure 5. Averaged Wall and Fluid temperature in microchannel structure

In addition to above results, in order to compute the wall temperature at each Z-location, some more calculations will be required. During fluid flow, water is in touch with four surfaces of these channels. It should be indicated that the above surface of this channel is assumed adiabatic. So, for calculation of wall temperature at each Z-location, this following equation, equation 11, will be utilized:

$$T_{wall-average} = \frac{T_{side-wall1} + T_{bottom-wall} + T_{wall-side2}}{3} \quad (11)$$

After calculation of averaged local temperature at each Z-location, heat transfer coefficient and averaged Nusselt number (Nu_{avg}) will be obtained from these following equations:

$$h(x) = \frac{q''}{\Delta T_m} \quad (12)$$

$$Nu_{avg} = \frac{hD_h}{k} \quad (13)$$

where ΔT_m is the log mean temperature difference, determined from:

$$\Delta T_m = \frac{\Delta T_{in} - \Delta T_{ex}}{\ln(\Delta T_{in}/\Delta T_{ex})} \quad (14)$$

A comparison between numerical results and Peng and Peterson's experimental Study [18] was occurred and the calculation of their differnces was performed and finally those obtained results are listed in Table 3. In order to compute the accuracy value at each simulation, the differnce percentage of each simulation is calculated individually.

Besides, the trend of variations of averaged Nusselt number in comparison with Reynolds number is shown in Figure 6. Also, the comparison of this numerical results with Peng and Peterson's experimental Study [18] is illustrated clearly.

TABLE 3. Averaged numerical and experimental Nusselt numbers and difference percentage at each simulation

Exp	Re_{Dh}	$Nu_{avg,exp}$	$Nu_{avg,num}$	Difference %
1	200	1.85	1.93	4.15
2	225	1.99	2.00	0.5
3	250	2.13	2.15	0.9
4	275	2.27	2.22	2.2
5	300	2.42	2.46	1.6

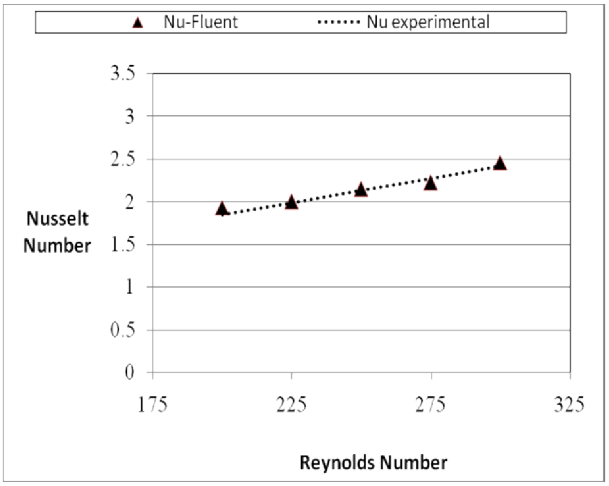

Figure 6. Averaged numerical and experimental Nusselt numbers in microchannel structure

As it can be seen in Figure 6 and Table 3, these numerical results are in an acceptable conformity with Peng and Peterson's available experimental study [18]. Between this indicated experimental study (equation 1) and averaged Nusselt number which is obtained in Fluent CFD Solver a differnce percentage in the range of 0.5 to 4.15% is existed.

3.2 Microchannels Pressure Drop In this section, variation in pressure values along the Z direction of microchannel has been investigated for five different Reynolds numbers. Like previous section, plate 3's geometry within the Reynolds number range of 200 to 300 was used in this numerical simulation. The trend of pressure changes along the Z direction of microchannel can be observed in Figure 7.

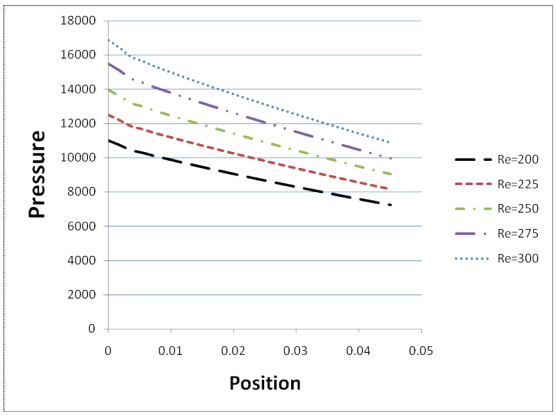

Figure 7. Variation in pressure values along the Z direction

Since a sudden flow contraction and expansion existed at the entrance and exit of the microchannels, the actual measured pressure drop included these contraction and expansion losses. The pressure drop, in Figure 7, however, represents the pressure drop only along the microchannels, hence, the calculated pressure drop caused by the contraction and expansion were subtracted from the measured values. Meanwhile, according to five different Reynolds number, to have better comparison, pressure drop values at each simulation has been shown in Figure 8.

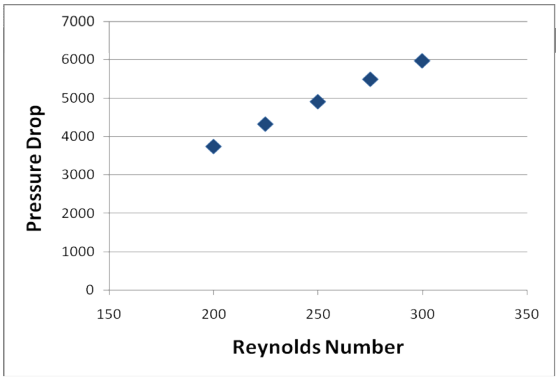

Figure 8. Pressure drop values at each Reynolds number

As it can be observed in Figure 8, the values for pressure drop will increase with increasing the Reynolds number. Further investigation showed that these trends were to be true for a wide range of Reynolds numbers in the region of laminar flow.

3.3 Effects Of Geometric Configurations On Laminar Heat Transfer Based on Peng and Peterson's study [18], twelve different microchannel structures were shown in Table 4. In order to compare and explore the effect of various channel dimensions on Nusselt number in laminar heat transfer, twelve different microchannels were simulated in this numerical study.

TABLE 4. Geometric parameters of the simulated models

Plate	W mm	W_c mm	W_t mm	L mm	H mm	D_h mm	$\frac{D_h}{W_c}$	$\frac{H}{W}$
1	0.4	4.5	18	45	0.2	0.267	0.0593	0.5
2	0.4	2.8	18	45	0.3	0.343	0.1225	0.75
3	0.4	2.0	18	45	0.3	0.343	0.1715	0.75
4	0.3	4.6	18	45	0.2	0.24	0.0533	0.667
5	0.3	2.8	18	45	0.3	0.3	0.1070	1.00
6	0.3	2.0	18	45	0.3	0.3	0.15	1.00
7	0.2	4.5	18	45	0.2	0.2	0.0444	1.00
8	0.2	2.8	18	45	0.3	0.24	0.0857	1.5
9	0.2	2.0	18	45	0.3	0.24	0.12	1.5
10	0.1	4.5	18	45	0.2	0.133	0.0296	2.0
11	0.1	2.8	18	45	0.3	0.15	0.0536	3.0
12	0.1	2.0	18	45	0.3	0.15	0.075	3.0

Figures 9, 10 describe the numerical results for the individual microchannel structures as a function of D_h/W_c and H/W on Nusselt number in laminar heat transfer.

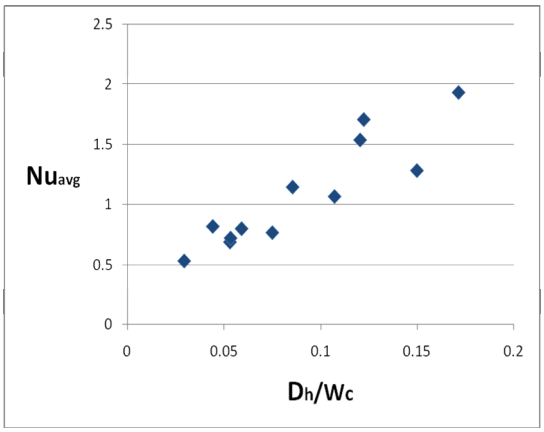

Figure 9. Effect of D_h/W_c on averaged Nusselt number in laminar heat transfer

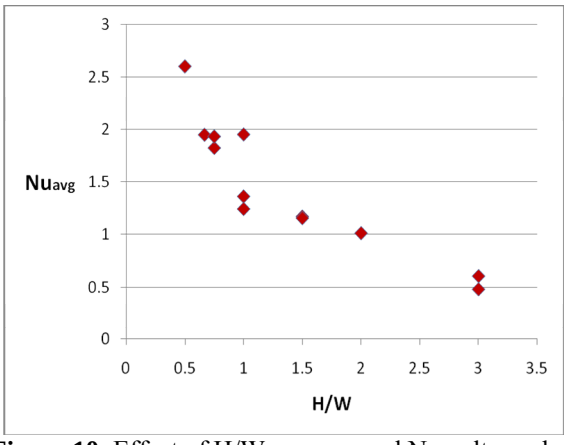

Figure 10. Effect of H/W on averaged Nusselt number in laminar heat transfer

It should be considered that all of the simulations in this section were performed when the Reynolds number was 200. Figure 9 indicates that the laminar heat transfer will increase by enlarging the hydraulic diameter or decreasing the center to center distance of microchannels. Figure 10 indicates that increasing the width or decreasing the height of the microchannel enhances the averaged Nusselt number in laminar heat transfer. With more consideration in other Reynolds number on laminar heat transfer, it was found that these trends were to be true for a wide range of Reynolds number.

4. CONCLUSIONS

- The differences between computational Nusselt number in this numerical simulation and available experimental studies were in a differnce percentage in the range of 0.5 to 4.15%.

- Variation in pressure values along the Z direction of the microchannel has been investigated for five different Reynolds number and it was concluded that the values for pressure drop will increase with increasing the Reynolds number.

- Numerical measurements in these simulations indicated that the geometric configurations of the microchannel structure and individual microchannels has a significant effect on the single phase convective heat transfer in laminar flow.

- In these simulations, it was specified that the averaged Nusselt number in laminar heat transfer does depend on the parameters D_h/W_c and H/W.

- The averaged Nusselt number in laminar heat transfer will increase by enlarging the hydraulic diameter or decreasing the center to center distance of microchannels.

- Increasing the width or decreasing the height of the microchannel enhances the averaged Nusselt number in laminar heat transfer.

5. REFERENCES

1. Keogh, A., "Microchannel heat exchangers", ***IEA. Heat Pump Centre***, Vol. 25, No. 3, (2007), 15-17.
2. Tuckermann, D.B. and Pease, R.F., "Optimized convective cooling using micro machined structure", ***Journal of the Electrochemical Society***, Vol. 129, No. 3, (1982), 98.
3. Tuckerman, D.B. and Pease, R.F., "High-performance heat sinking for VLSI", ***IEEE Electron device Letters***, Vol. EDL-2, (1991), pp.126-129.
4. Wu, P.Y. and Little, W.A., "Measurement of friction factor for the flow of gases in very fine channels used for micro miniature Joule-Thompson refrigerators", ***Cryogenics,*** Vol. 23, No. 5, (1983), 273-277.
5. Wu, P.Y., and Litle, W.A., "Measurement of the heat transfer characteristics of gas flow in fine channels heat exchangers used for micro miniature refrigerators", ***Cryogenics,*** Vol. 24, No. 8, (1984), 415-420.
6. Choi, S.B., Barron, R.F. and Warrington, R.O., "Liquid flow and heat transfer in microtubes, In Micromechanical Sensors, actuators and systems", ***Dynamic systems and control division***, Vol. 32, (1991), 123-134.
7. Weisberg, A., Bau, H.H. and Zemel, J., "Analysis of microchannels for integrated cooling", ***International Journal of Heat and Mass Transfer,*** Vol. 35, No. 10, (1992), 2465-2474.
8. Bowers, M.B. and Mudawar, I., "High flux boiling in low flow rate, low pressure drop minichannel and microchannel heat sinks", ***International Journal of Heat and Mass Transfer***, Vol. 37, No. 2, (1994), 321-332.
9. Peng, X.F., and Wang, B.X., "Experimental investigation on flow boiling of liquid through microchannels", ***Chinese Journal of Engngineering Thermophys***, Vol. 14, No. 3, (1993), 281-286.
10. Peng, X.F., Wang, B.X., Peterson, G.P. and Ma, H.B., "Experimental investigation of heat transfer in flat plates with rectangular microchannels", ***International Journal of Heat and Mass Transfer***, Vol. 38, No. 1, (1995), 127-137.
11. Peng, X.F. and Peterson, G.P., "The effect of thermofluid and geometrical parameters on convection of liquids trough rectangular microchannels", ***International Journal of Heat and Mass Transfer***, Vol. 38, No. 4, (1995), 755-758.
12. Peng, X.F. and Peterson, G.P., "Frictional flow

characteristics of water flowing through rectangular microchannels", ***Journal of Experimental Heat and mass transfer,*** Vol. 7, No. 4, (1995), 249-264.
13. Peng, X.F., Peterson, G.P. and Wang, B.X., "Heat transfer characteristics of water flowing through microchannels", ***Journal of Experimental Heat and mass Transfer,*** Vol. 7, No. 4, (1995), 265-283.
14. Qu, W. and Mudawar, I., "Analysis of three-dimensional heat transfer in microchannel heat sinks", ***International Journal of Heat and Mass Transfer***, Vol. 45, No. 19, (2002), 3973-3985.
15. Peng, X.F., Piao, Y. and Jia, L., "Single-phase convective heat transfer in microchannels", ***Progress in Natural Science***, Vol. 12, No. 10, (2002), 721-728
16. Owhaib, W. and Palm, B., "Experimental investigation of single-phase convective heat transfer in circular microchannels", ***Experimental Thermal and Fluid Science***, Vol. 28, No. 2-3, (2004), 105-110.
17. Mokrani, O., Bourouga, B., Castelain, C. and Peerhossaini, H., "Fluid flow and convective heat transfer in flat microchannels", ***International Journal of Heat and Mass Transfer***, Vol. 52, No. 5-6, (2009), 1337-1352.
18. Peng, X.F. and Peterson, G.P., "Convective heat transfer and flow friction for water flow in microchannel structures", ***International Journal of Heat and Mass Transfer***, Vol. 39, No. 12, (1996), 2599-2608.
19. Incropera, F.P., DeWitt, D.P., Bergman, T.L. and Lavine, A.S., Introduction to Heat Transfer, Fifth edition. Wiley, Newyork, (2007).